BJRS
BRAZILIAN JOURNAL OF RADIATION SCIENCES

doi.org/10.15392/2319-0612.2024.2424
2024, 12(2) | 01-22 | e2424
Submitted: 2024-01-23
Accepted: 2024-06-04

Doses associated with interventional radiology patients: a retrospective analysis in cerebral angiography

Assimos [a*], R. N.; Canevaro [b], L.V.

[a] Universidade Federal do Rio de Janeiro /UFRJ/ Instituto de Física, 21941-909, Rio de Janeiro, RJ, Brazil.
[b] Instituto de Radioproteção e Dosimetria/IRD/Divisão de Física Médica, 22783-127, Rio de Janeiro, RJ, Brazil.

*Correspondence: assimosraquel@gmail.com; lucia.canevaro@ird.gov.br

Abstract: Interventional Radiology (IR) plays a major role in neurology. It has several advantages, such as avoiding higher risk surgeries and reducing hospital stay. IR allows the diagnosis of various diseases, such as strokes, neurological dysfunctions, arteriovenous malformations, etc. Despite its advantages, IR delivers high radiation doses to patients, mainly due to long exposure times and the large number of images acquired (cine or DSA mode). In this work, a retrospective study was carried out using information from cerebral arteriography procedures (CAP) recorded in the IRaD (Interventional Radiology Database). Data were extracted from 39 procedures to analyze the frequency of the C-arm X-ray machine projections performed during the procedures and the contribution of the different projections of the C-arm to air kerma and air kerma/image parameters in DSA mode, and this has been done at various angles and for the most commonly used filters. The mean values and standard deviations of total air kerma area product (PKA) and air kerma at the patient entrance reference point (Ka,r) were (7584 ± 4661) μGy·m^2 and (746 ± 378) mGy, respectively. It was verified that the total dose delivered to the patient is mainly composed of the dose due to the exposure in DSA mode. In the different C-arm projections during DSA, it was found that the greater the angle of the C-arm (more horizontal), the smaller the air kerma/image value. Also, the more cranial the projection, the greater the air kerma/image value. In the most frequent projections, the equipment was programmed to deliver the lowest doses to the patient by inserting additional copper and aluminum filters.

Keywords: Interventional Radiology, arteriography, radiation dose, neurology.

BJRS
BRAZILIAN JOURNAL OF RADIATION SCIENCES

doi.org/10.15392/2319-0612.2024.2424
2024, 12(2) | 01-22 | e2424
Submitted: 2024-01-23
Accepted: 2024-06-04

Doses de radiação associadas a pacientes em radiologia intervencionista: uma análise retrospectiva em angiografia cerebral

Resumo: A Radiologia Intervencionista (RI) desempenha um papel importante na neurologia. Possui várias vantagens, tais como evitar cirurgias de maior risco e reduzir o tempo de hospitalização. A RI permite diagnosticar várias doenças, como acidentes vasculares cerebrais, disfunções neurológicas, malformações arteriovenosas, etc. Apesar das suas vantagens, a RI fornece doses elevadas aos pacientes, principalmente devido aos longos tempos de exposição e ao grande número de imagens adquiridas (modo cine ou DSA). Neste trabalho, foi feito um estudo retrospectivo utilizando informações de procedimentos de arteriografias cerebrais (PAC) registadas na base de dados IRaD (Interventional Radiology Database). Foram extraídos dados de 39 procedimentos visando analisar: a frequência das projeções do equipamento arco em C durante os procedimentos; a contribuição das diferentes projeções do arco em C para os parâmetros kerma no ar e kerma/imagem em DSA em vários ângulos e para os filtros mais utilizados. Os valores médios e os desvios-padrão do produto kerma área total (PKA) e do kerma no ar no ponto de referência de entrada do paciente (Ka,r) foram (7584 ± 4661) μGym^2 e (746 ± 378) mGy, respectivamente. Verificou-se que a dose total administrada ao paciente é composta principalmente pela dose devida à exposição em modo DSA. Nas diferentes projeções do arco em C durante DSA, verificou-se que quanto maior o ângulo do arco em C (mais horizontal), menor o valor de kerma/imagem. Da mesma forma, quanto mais cranial a projeção, maior o valor kerma/imagem. Nas projeções mais frequentes, o equipamento foi programado para fornecer doses mais baixas ao paciente, inserindo filtros adicionais de cobre e alumínio.

Palavras-chave: Radiologia Intervencionista, angiografia, dose de radiação, neurologia.

SBPR

1. INTRODUCTION

Interventional Radiology can be defined as "procedures comprising guided therapeutic and diagnostic interventions, by percutaneous or other access, usually performed under local anesthesia and/or sedation, with fluoroscopic imaging used to localise the lesion/treatment site, monitor the procedure, and control and document the therapy". Among its advantages, the main ones being the avoidance high risk surgeries and long hospital stays, thus reducing surgical cuts, likelihood of infections and hospital costs. [1,2]

Interventional radiology plays a major role in neurology. Neuroradiology is a subspecialty of radiology that is especially dedicated to the diagnosis or treatment of possible abnormalities in the brain, spinal cord and head and neck. The practice consists of a minimally invasive technique in which the doctor introduces a catheter and a guide wire through an incision that can be femoral, radial or brachial, using a contrast medium and ionizing radiation to locate the lesion. Radiopaque contrast media are substances of high physical density that are used to help delineate the borders between tissues with similar radiodensity and thus facilitate the identification of lesions or pathologies. These techniques are used to diagnose various diseases, such as strokes, neurological dysfunctions, aneurysms, Alzheimer's disease, among others [3, 4].

Digital Subtraction Angiography (DSA) is a gold standard diagnostic method for assessing aneurysms, which also detects other diseases such as tumors, strokes and malformations [5]. It consists of obtaining a sequence of images of the blood vessels before (mask) and another sequence after a radiopaque contrast medium is injected. One image sequence is then computationally subtracted from the other. This eliminates images of structures other than arteries. This allows the blood vessels to be highlighted, thus enabling an efficient diagnosis [6, 7]. During a given procedure, the patient is exposed to radiation in

two ways: In fluoroscopy mode, which consists of irradiation in real time, without the observed images being stored, and in DSA mode, in which case the images are recorded in the C-arm X-ray machine's memory.

Despite its great advantages, interventional radiology is one of the applications of X-rays that delivers the highest radiation doses to patients, and in some cases can cause radio-induced injuries [8, 1, 9]. These effects are due to long exposure times, high dose rates, high number of cine/DSA images acquired, as well as the use of collimators and filters, C-arm projections, among other factors. [2]

IRaD is a database created by our research group in order to store all the information of cardiology and neuroradiology procedures collected in interventional radiology departments of many hospitals where we have been working. The information includes data on the procedure such as type, total fluoro time (FT), C-arm projections in cine/DSA mode, radiographic techniques, etc, as well as patient and staff information (PKA, Ka,r, Hp(d), etc.). [10]

In Brazil, following various international recommendations [11, 12, 13, 8], the RDC (Resolution of the Board of Directors) 611/2022 [14] establishes that "all procedures performed in diagnostic or interventional radiology services must comply with the principles of justification, optimization, dose limitation and accident prevention, in order to ensure that patient exposure to the inherent risks of each technology is the minimum necessary to guarantee patient safety and the expected quality of images and procedures". Furthermore, RDC 611 determines the implementation of quality assurance programs, as well as the optimization of medical exposures to the minimum value necessary to obtain the radiological objective, taking into account diagnostic reference levels.

In this scenario, to analyse patient doses is extremely relevant. For this purpose, the frequency of the various radiological projections performed during cerebral arteriography procedures (CAP), air kerma area product (PKA) and air kerma at the patient entrance reference point (Ka,r) magnitudes were studied. In relation to the patient entrance reference point, the

percentage of air kerma due to the DSA series was evaluated, taking into account all the different C-arm projections used. The kerma/image value in the most used projections during the procedures was also investigated, as well as the copper and aluminum filters influence.

The primary objective of this study was to identify the projections that result in higher radiation doses to patients. Accordingly, we investigated the variation in kerma/image across different projections, since the number of images acquired for a given projection can vary between cases.

2. MATERIALS AND METHODS

This study used information stored in the IRaD database on neuroradiology procedures carried out in a specialized hemodynamic department. Data was randomly extracted from 39 stored CAP which were carried out by the same medical and technical team in 2018.

The x-ray unit used was a SIEMENS Artis Zee floor, with a C-arm and a 20 x 20 cm flat panel image detector system. All procedures were carried out in the normal mode of exposure rate. At the end of each CAP, the C-arm X-ray machine provided a structured report of the procedure steps. Information about fluoro techniques is not recorded in this report. The recorded series were obtained with the DSA technique in the 39 procedures evaluated. In fluoroscopy mode, the equipment automatically introduces additional filtration, in millimeters of copper (mmCu), according to the patient's thickness and other parameters set by the manufacturer. In DSA mode, the equipment introduces combinations of aluminum and copper filters in response to a more complex logic, depending on various parameters such as FT, number of series acquired, work protocols, etc.

2.1. Analysis of both fluoro and DSA parameters

With the aim of studying the distribution of the different parameters that form part of the exam and their influence on the dose administered to the patient, in a first step, were analysed the total values of the quantities, considering together the fluoroscopic contributions (exposure in real time, not recorded) and DSA (acquired, recorded series). The following analyses were carried out:

- total FT for each procedure;
- percentage relation between subtraction (DSA) PKA and fluoro PKA values in relation to the total PKA value (DSA+fluoro);
- percentage relation between the DSA kerma and fluoro kerma values in relation to the total kerma value (DSA+fluoro).

2.2. Analysis of DSA parameters

The next step of the research was to carry out an analysis in terms of dose delivered, considering only the DSA series acquired in all procedures. Thus, the different projections in DSA mode in which patients are irradiated during procedures were identified. The following analyses were then carried out:

- Calculation of the kerma/image for each series and each projection;
- Comparison of kerma/image between different projections.

In order to identify the angles (and their frequency) used to acquire the DSA series in CAP, data from all the series acquired in the 39 procedures were organized in a single spreadsheet. On the x-ray equipment´s monitors, the projection being used are displayed according to the inclination of the x-ray tube-detector axis to the left or right of the patient, as being left anterior oblique (LAO) or right anterior oblique (RAO), respectively. The

inclination of this axis in cranial (CRAN) or caudal (CAU) orientation is showed as well. The DSA projections were organized into 4 categories:

- LAO-CRAN;
- LAO-CAU;
- RAO-CRAN;
- RAO-CAU.

Figure 1 shows the projections of the C-arm on a fluoroscopy device.

Figure 1: C-arm projections on a fluoroscopy device. [15]

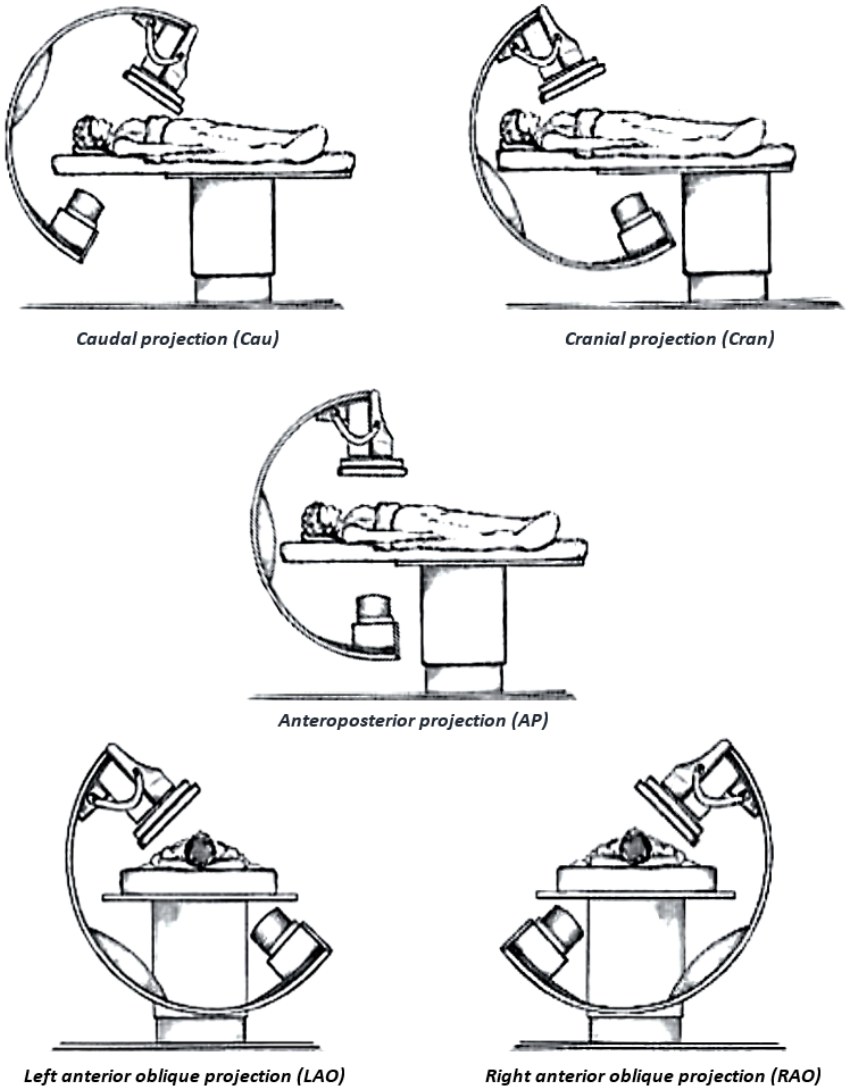

Due to the uncertainty in the displacement and positioning of the X-ray tube-image detector axis, projection ranges varying by 10 degrees were considered. For example, a series acquired at position (LAO 33-CRAN 12) was classified as LAO 30-CRAN 10. This methodology allows the projections to be organized into groups, making it easier to visualize and optimize the observations. In addition, all the projections were counted (number of times each projection appeared in the sample of 39 procedures studied) and organized from highest to lowest frequency. When all the projections obtained from the 39 examinations were put together, a set of 507 projections was obtained. As a result of this methodology, the projections were organized according to the four categories considered and their frequency in the sample of 39 procedures studied (N).

Of the total of 507 projections, 55 (10% of the total) were excluded due to their low frequency, because these were performed exceptionally and do not represent projections normally used in a typical cerebral angiography procedure.

Next, projections representing the same position of the X-ray tube-detector axis were grouped together. For example, the angles LAO 0-CRAN 0, LAO 0-CAU 0, RAO 0-CRAN 0 and RAO 0-CAU 0 represent the same position as the X-ray tube and are therefore the same. They were named anteroposterior (AP).

Likewise, LAO 90 - CRAN 0 and LAO 90 - CAU 0 represent the same projection, which we'll call LAO 90. The same procedure was carried out for the other projections.

After this reorganization, Table 1 showing the most frequent projections was drawn up, including all the projections.

Table 1: Group of projections considered. (N: number of times each projection appeared in the sample of 39 procedures studied).

PROJECTION	N
RAO 90	87
LAO 90	77
LAO 0 - CRAN 10	55
LAO 30	52
RAO 30	51
AP	44
RAO 0 - CRAN 10	35
LAO 0 - CRAN 20	17
RAO 20	14
LAO 20	12
RAO 40	8
TOTAL	452

2.3. Statistical analysis

The analysis of variance (ANOVA) is used to compare the means of a numerical random variable in more than two populations. The numerical variable whose means are being compared in three or more populations is called the response or the dependent variable. The categorical variable that distinguishes the various populations under study is called the treatment, factor, explanatory variable, or independent variable.

In this study, the dependent variable to be analysed is the kerma/image and the independent variable is projection. ANOVA was therefore carried out to compare the kerma/image means of the different projections groups.

Analysing the assumption of data normality, the Shapiro-Wilk test was used to verify whether the sample distribution is normal. In order to do so, the null hypothesis (H_0) is

considered, which represents when the data analysed is normal and H_1 when it is not. If there is no normal distribution, it is still valid to carry out the test despite not agreeing with one of the assumptions, since ANOVA is a robust test and is still applicable in these cases. [16] Therefore, the robustness of ANOVA should be taken into account for deviations from normality and equality of variances that are not too marked. [17]

When we reject H_0 in the ANOVA, we can conclude that there is at least one population mean that is significantly different from the others. However, ANOVA does not indicate which pair or pairs of means are different. To specifically locate the difference, it was necessary to use the Tuckey test. This test compares the means pairwise, called a multiple comparison of means. When regarding deviations from normality and homogeneity of variances on tests, the Tuckey test is one of the most robust. [18]

To verify the ANOVA results, the Kruskal-Wallis test was used. This test is a non-parametric alternative to one-way ANOVA. It can be used to test two or more independent samples, indicating whether there is any difference in at least two of the groups studied. The groups must have a single continuous variable and there must be no normal distribution. [19,20]

3. RESULTS AND DISCUSSIONS

3.1. Analyses of total sample parameters

Table 2 shows a summary of the values of the quantities resulting from a total of 39 CAP. Numerical values of the quantities PKA and Ka,r were extracted from the database and had already been corrected for the C-arm X-ray machine.

Table 2: Values of the parameters extracted from the sample used in this work.

	MEAN + SD	MEDIAN	3°Q	MAX - MIN
Number of series	13 ± 5	14	17	23 - 3
Number of images/procedure	409 ± 241	353	619	1065 - 87
Total FT (minutes)	6,4 ± 3,6	5,7	8,3	15,9 – 1,2
DSA PKA, PKA_{st} (µGy.m²)	6975 ± 4395	7346	9018	23270 - 1437
Fluoro PKA, PKA_{ft} (µGy.m²)	609 ± 500	467	792	2243 - 92
Total PKA, $PKA_{(f+s)}$ (µGy.m²)	7584 ± 4661	7776	9803	23892 -1552
Kerma (DSA) series, K_{st} (mGy)	689 ± 349	735	890	1684 - 210
Fluoro Kerma, K_{ft} (mGy)	58 ± 48	43	65	195 - 8
Total kerma, $K_{(f+s)}$ (mGy)	746 ± 378	780	964	1878 - 225

The large standard deviation (SD) values and the wide range between maximum and minimum values are due to the variability of pathologies, particularities in the anatomy of the arteries of the patients, difficulties in carrying out the procedure when transiting with the catheter, and the high complexity of the procedures, among other reasons. This situation is inherent to interventional practice and cannot be changed, and it is not possible to reduce the spread of the SD.

3.1.1. Kerma-Área Product (PKA)

In order to ascertain the contributions of PKA in fluoro and DSA modes at the patient entrance reference point, the values for total PKA, fluoro PKA and DSA PKA were calculated, as shown in Table 4. On average, 91.97% of total PKA is due to exposure in DSA mode (Figure 2). It can be seen that subtraction PKA contributes to most of the total PKA, while fluoro PKA represents a small contribution to the total PKA.

Figure 2: Representation of PKA's partial and total contributions.

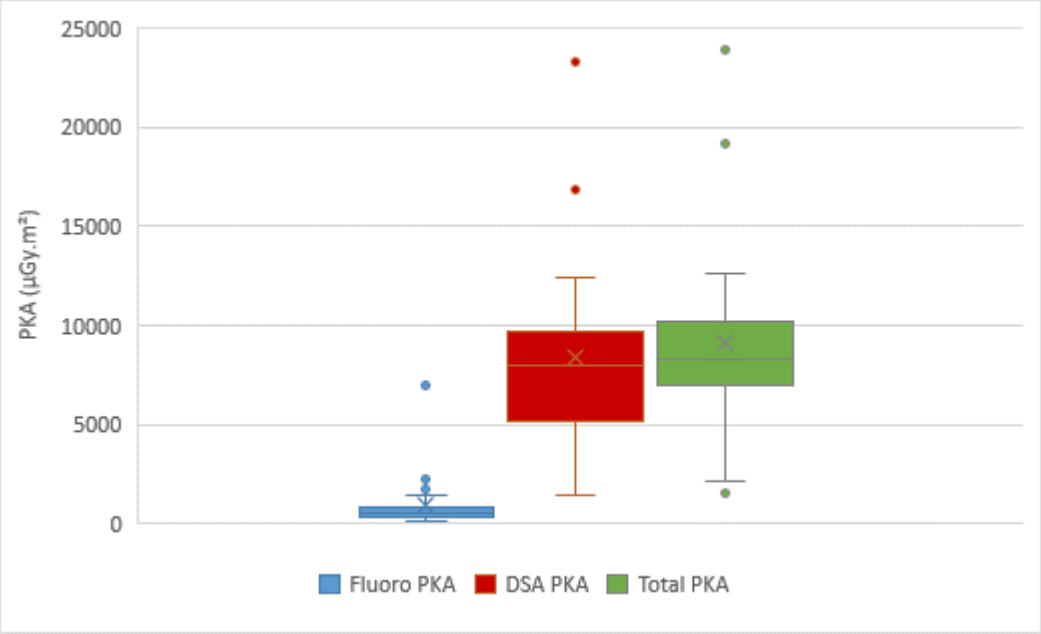

Comparing the values of total PKA, cine and fluoro in this study with those of other articles found in the literature, we can affirm that the results found in this study are consistent with those compared, maintaining the same behavior in presenting a predominance of DSA PKA. For example, the study by Bor at al. (2006) [21] showed an 81.74% share of DSA PKA, with a mean value of 7480 μGym^2 and a mean value of fluoro PKA of 1670 μGym^2. The same happens in another study by Bor at al. (Bor, 2004) [22] in which the contribution of DSA PKA represented 93% of the total, in which it has average values of DSA PKA and of fluoro PKA of, respectively, 7960 and 600 μGym^2.

3.1.2. Air kerma at the patient entrance reference point (kerma)

As with the PKA analysis, the DSA, fluoro and total kerma values were assessed (Table 2). In this case, an average of 92.33% of total kerma is due to an exposure in DSA mode, as can be seen in Figure 3.

Figure 3: Representation of the partial and total contribution of kerma.

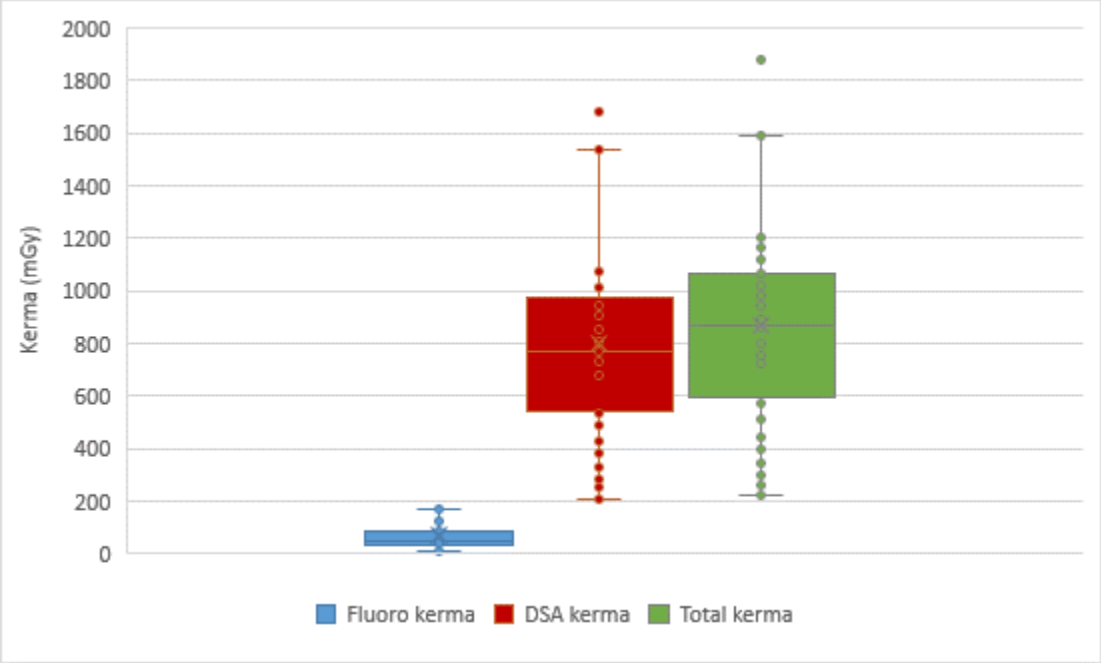

Comparing the total, DSA and fluoro kerma values of this study with those of other articles found in the literature, we can affirm that the results found in this paper are consistent with the comparisons, showing the same behavior in presenting a greater predominance of DSA kerma. For example, in the study by Lunelli et al (2013) [23], the DSA kerma is within the order of the uncertainties of the present study, with a value of (626±32) mGy, and the fluoro kerma with a value of (110±8.9) mGy.

3.2. Kerma/image analysis for the different projections in DSA mode

Based on the above observations, only the DSA mode results were analysed in the present work. Although the DSA series last for short periods of time (in the order of a few seconds), it is clear that this portion of the dose that the patient receives is the most relevant, added to the fact that the values measured at the patient's entrance reference point are, on average, in the order of 0.5 Gy.

The main objective of this study was to identify those projections in which the patient receives higher doses. Thus, we studied how the kerma/image value varies in the

different projections, since the number of images acquired for a given projection varies from one case to another.

Figure 4 shows a bar chart showing the most frequent projections used by professionals (represented by the blue bars). The same figure also shows the average value of kerma/image in mGy (multiplied by 10 for better visibility), which the orange bars show.

The views that result in the highest kerma/image value for the patient are LAO 0 - CRAN 20 and RAO 20. Although these angles result in greater kerma/image, they are not used very often daily during procedures. On the other hand, we see that the RAO 90 and LAO 90 views, which appeared 87 and 77 times respectively over the course of the 39 procedures, are the most used by professionals, have a large number of images, and the ones that cause the lowest kerma/image (around 0,7 mGy in the projection RAO 90 and 1,3 mGy in LAO 90).

Figure 4: Bar graph showing the frequency of projections used during the procedures.

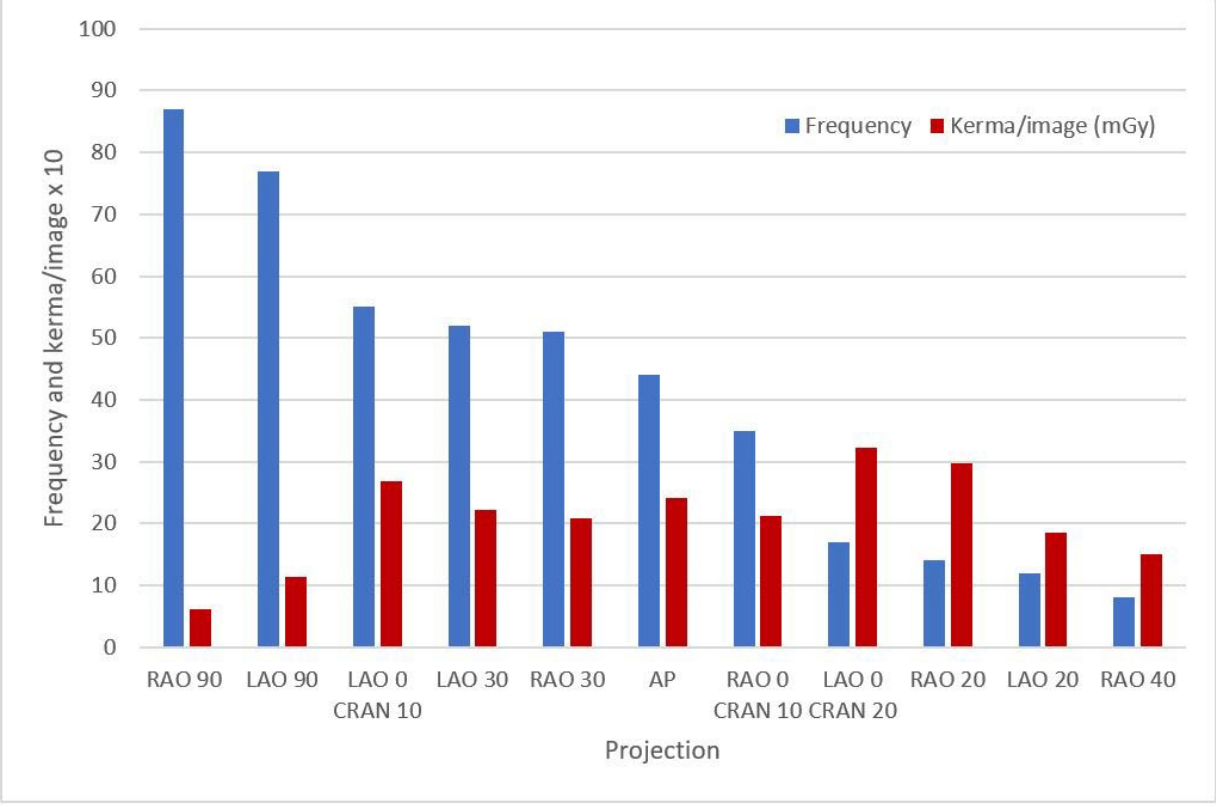

3.3. Statistical analysis of the results

Looking at Figure 5, we can infer a tendency for the kerma/image values of the RAO 90 and LAO 90 projections to be grouped together (Group 1), since the median and third quartile kerma/image values are close, with the median ranging from 0.5 to 1.5. Using the same criteria, two more groups were identified: Group 2, with medians ranging from 2 to 3, and Group 3, with medians above 3. Grouping according to median was necessary due to the large number of outliers present.

Therefore, the projections were grouped as follows (Figure 4):

- Group 1 - LAO 90 and RAO 90;
- Group 2 - LAO 0 CRAN 10, RAO 0 CRAN 10, AP, LAO 30, LAO 20, RAO 30, RAO 40;
- Group 3 - LAO 0 CRAN 20 and RAO 20.

Figure 5: Identification of groups 1, 2 and 3.

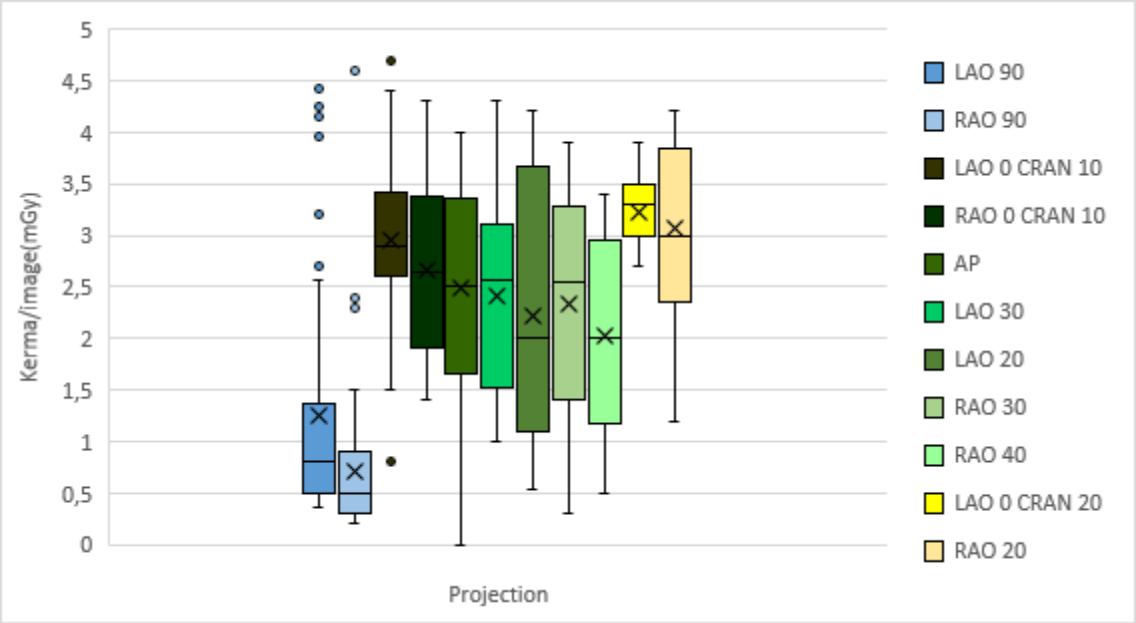

In order to carry out a less qualitative analysis and to unify the projections with similar mean and median values, rather than having to study them individually, the ANOVA test was applied to compare the mean kerma/image values of the groups formed previously according to the analysis in Figure 5.

With regard to the normality of the data, the p-values for groups 1, 2 and 3 were, respectively 2.65×10^{-16}, 2.19×10^{-12}, 1.15×10^{-7}. In this case, all the groups have a p-value lower than the significance level considered (0.05), thus rejecting the null hypothesis. This means that the data does not follow a normal distribution. The same is true for the incidences in groups 2 and 3.

When analyzing the results of the ANOVA test, as shown in Table 3, the variation of the mean square is much greater than the mean square within the same group (residual). So we have that on average there is at least one difference between one of the different groups, resulting in an F value of 107.90, considering H_0 = the means values of the groups are the same, and H_1 = the means values of the groups are different.

Next, when we check the p-value, considering the significance level as 0.05, we see that it is lower than the level adopted. This means that there is at least one difference between the two mean values involved in the groups, which are statistically different from zero. Therefore, one group's kerma/image value is higher than another group's projection.

Table 3: ANOVA test results.

KERMA/IMAGE (mGy)	MEAN SQUARE	F VALUE	P-VALUE
Groups 1, 2 and 3	127,41	107,90	$<2\times e^{-16}$
Residual	1,18	-	-

To check which mean values differed from each other, a multiple comparison procedure was carried out, using the Tuckey test. It can therefore be concluded that there is a statistically significant difference between groups 1 and 2, since the p-value is less than

0.0001, the significance level adopted. Therefore, H_0 is rejected. The same result was seen when comparing the mean values between groups 3 and 1 and between groups 3 and 2.

As the data does not have a normal distribution, the Kruskal-Wallis non-parametric test was carried out to verify the results of the analysis of variance. The p-value found was 2, $2\times e^{-16}$, leading to the conclusion that at least 2 groups are different from each other, thus confirming the result found through ANOVA.

It can therefore be concluded that the kerma/image values between groups 1, 2 and 3 are statistically different and that there is therefore a difference in kerma/image when varying the incidences considered.

A second conclusion based on the results of the ANOVA test is that the LAO 90 and RAO 90 projections can be grouped together (group 1) when studied and that they have the lowest kerma/image value of all the projections analysed. With regard to groups 2 and 3, all the incidences in these groups can also be studied together, as their kerma/image values are close. The contribution of the kerma/image value of group 2 incidences to the patient is intermediate. On the other hand, LAO 0-CRAN 20 and RAO 20 projections (group 3) result in a higher dose, since the kerma/image of this group is high.

3.4. Effect of automatic insertion of aluminum and copper filters on patient dose

Figure 6 shows the sequence of DSA series acquired during a particular cerebral arteriography procedure; 21 series were acquired, with the projections represented on the horizontal axis of the graph according to the time sequence in which the exam was carried out.

Figure 6: Performance of aluminum and copper filters during one cerebral arteriography procedure.

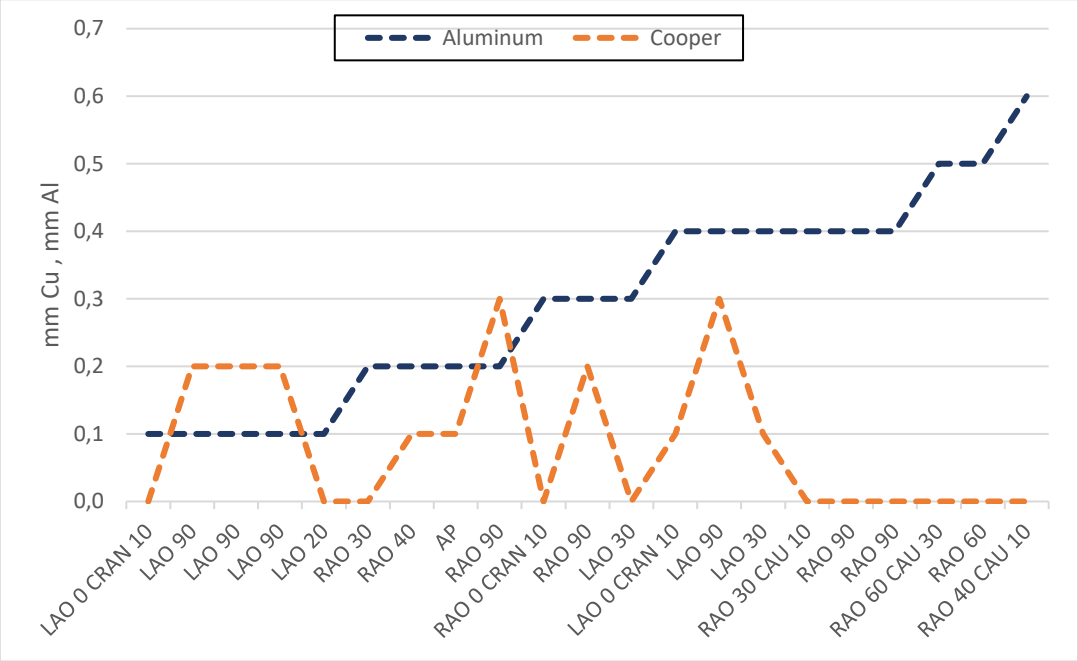

It can be seen that the thickness of the aluminum filters increases as more series are acquired. In other words, as the dose delivered to the patient increases, the x-ray equipment inserts more filtration. On the other hand, the thickness of the copper filters inserted is greater for highly angled incidences; it is particularly heavy for extreme angles such as 90 degrees. This process takes place until a certain point when the degree of aluminum filtration is very significant, and the equipment no longer inserts copper filters. In almost all the procedures, this way of filter insertion was similar.

The CARE package (**C**ombined **A**pplications to **R**educe **E**xposure) is a dose reduction software that is used in the procedures carried out in this study. It helps to reduce radiation dose for the operator and the patient. Included in this package is the CARE filter package, which automatically selects the copper filters. This filter removes the low-energy components of the X-ray spectrum that are not needed to create the image, thereby reducing the dose. [24] Filter insertion is managed by the C-arm machine's automatic exposure control, depending on various parameters such as FOV (Field Of View), SID (Source-Image

Distance), contour filters, etc. The authors are not aware of all the parameters that control this filter insertion algorithm, but the maximum aluminum thickness observed over the 39 procedures evaluated was 0.9 mm. No more filters were added after this value.

4. CONCLUSIONS

It was found that, during CAP, the largest portion of the total dose received by the patient is due to the irradiation during DSA imaging (kerma at the patient entrance reference point and kerma-area product). Total values observed in the PKA and kerma records at the patient entrance reference point during the 39 CAP were, respectively, (7584 ± 4661) $\mu Gy.m^2$, with a third quartile of 792 $\mu Gy.m^2$, and (746 ± 378) mGy, with a third quartile of 964 mGy.

With regard to the variation in the kerma/image value in the different projections, it was found that the projections that provide a higher kerma/image value are not used very often, such as LAO 0-CRAN 20 and RAO 20. On the other hand, the RAO 90 and LAO 90 angles are the most commonly used in daily CAP and, despite this, result in a lower dose. In short, the more horizontal the incidence, the lower the kerma/image value. On the other hand, the more "cranial" the angles, the higher the kerma/image values obtained.

Applying the ANOVA test, it was possible to create three groups including projections with similar mean and median kerma/image values (groups 1, 2 and 3). Thus, it was not necessary to study each projection individually. This methodology allowed us to conclude that the LAO 90 and RAO 90 projections form a group (group 1) and that they have the lowest kerma/image value of all the projections analysed. The same holds for groups 2 and 3, with the kerma/image value of the group 2 views for the patient being intermediate. On the other hand, those projections included in group 3 provide higher doses.

About the automatic insertion of copper and aluminum filters by the x-ray unit evaluated, it was observed that, at 90 degree angles, the thickness of the copper filters inserted

is significant, reaching up to 0.3 mm Cu. With regard to the insertion of aluminum filters, their thickness increases as the number of series acquired increases during the procedure. Once their thickness is sufficient, the copper filters are no longer inserted.

ACKNOWLEDGMENT

We thank the health professional team from Hospital IEC, Rio de Janeiro who provided insight and expertise that greatly assisted the research, although they may not agree with all of the conclusions of this paper.

This work was carried out in the Medical Physics Division of the Institute of Radioprotection and Dosimetry/National Nuclear Energy Commission, Rio de Janeiro, Brazil.

FUNDING

No funding sources.

CONFLICT OF INTEREST

All authors declare that they have no conflicts of interest.

REFERENCES

[1] ICRP, International Commission on Radiological Protection. **Avoidance of radiation injuries from medical interventional procedures**. ICRP Publication 85, Annals of the ICRP, v. 30 n. 2, Vienna 2000.

[2] CANEVARO, L. Aspectos Físicos e Técnicos da Radiologia Intervencionista. **Revista Brasileira de Física Médica**, v. 3, n. 1, p. 101-115, 2009.

[3] ASNR. O que é neurorradiologia. Available on the site: <https://www.asnr.org/patientinfo/whatisnr.shtml>. Accessed on: October 12, 2022.

[4] MARDEGAN, Flávia. **Interpretação quantitativa dos fatores associados à exposição ocupacional e de pacientes em neurorradiologia intervencionista**. 2020. 84 f. TCC (Graduação) - curso de física médica, Instituto de Física, Universidade Federal do Rio de Janeiro, Rio de Janeiro, 2020. Acesso em: janeiro de 2020.

[5] AZEVEDO, Brenda. et al. Angiografia cerebral: agente modificador no desfecho do diagnóstico de aneurismas cerebrais e em seu planejamento cirúrgico. **Brazilian Journal of health Review**, Brasil, v.2, n.4, p. 2990-2997, jul./ag.2019.

[6] A.K, Jones. et al. Fluoroscopic Imaging Systems. *In*: DR, Dance. **Diagnostic Radiology Physics**: A Handbook for Teachers and Students. Vienna: International atomic energy agency, 2014. p. 183-205. ISBN 978-92-131010-1.

[7] ANGIOGRAFIA. MSD Manual Family Health Version. Available on the site: <msdmanuals.com>. Accessed on: January 19, 2023.

[8] ICRP, International Commission on Radiological Protection. Radiological Protection in Medicine. **ICRP Publication 105**, Annals of the ICRP, v. 37, n. 6, 2007.

[9] Vano, E., Gonzalez, L., Guibelalde E., Aviles P., Fernandez, J. M., Prieto, C, and Galvan, C. **Evaluation of risk of deterministic effects in fluoroscopically guided procedures.** Radiation Protection Dosimetry. v. 117, n. 1–3, p. 190–194, 2005.

[10] CNPq. Certified group. dgp.cnpq.br/dgp/espelhogrupo/1543497898512376. Accessed on: August 20, 2021.

[11] ICRP, International Commission on Radiological Protection. **ICRP PUBLICATION 103: The 2007 Recommendations of the International Commission on Radiological Protection**, Annals of the ICRP, v.37, n.4, p. 1-339, 2007.

[12] European Union. DIRECTIVA 2013/59/EURATOM DEL CONSEJO de 5 de diciembre de 2013 por la que se establecen normas de seguridad básicas para la protección contra los peligros derivados de la exposición a radiaciones ionizantes, y se derogan las Directivas 89/618/Euratom, 90/641/Euratom, 96/29/Euratom, 97/43/Euratom y 2003/122/Euratom. **Official Journal of the European Communities**, L 13, p. 1-73, 2014.

[13] IAEA, International Atomic Energy Agency. Protocolos de Control de Calidad para Radiodiagnóstico en América Latina y el Caribe. IAEA TECDOC 1958, Vienna, 2021.

[14] BRASIL. Ministério da Saúde. Agência Nacional de Vigilância Sanitária (ANVISA). Resolução da Diretoria Colegiada – **RDC n° 611**, de 09 de março de 2022.

[15] ALOAN, L., Hemodinâmica e Angiocardiografia: obtenção de dados, interpretação e aplicações clínicas. São Paulo: Atheneu Rio. 1990.

[16] Blanca, M.J. et al. Non-normal data: Is ANOVA still a valid option? **Psicothema**, v.29, n.4, p. (552 - 557), 2017.

[17] FREIRE, SM. Bioestatística Básica. Livro eletrônico. Rio de Janeiro: Ed. do autor, 2021.

[18] Maroco,J. Análise Estatística: com utilização do SPSS. Terceira Edição. Lisboa: Edições Sílabo, 2007.

[19] https://www.inf.ufsc.br/~vera.carmo/Testes_de_Hipoteses/Teste_Nao_parametrico_Kruskal-Wallis.pdf. Accessed on: March 25, 2023.

[20] McKight, P.E.; Najab, J. Kruskal Wallis test. **The Corsini Encyclopedia of Psychology**. January 2010.

[21] BOR, B. et al. Patient and Staff Doses in Interventional Neurorradiology. **Radiation Protection Dosimetry**, v. 117, n. 1-3, p. (62-68), February 2006.

[22] BOR, D. et. al. Comparison of effective doses obtained from dose–area product and air kerma measurements in interventional radiology. **The British Journal of Radiology**, v. 77, vn. 916, p. (315-322), April 2004.

[23] LUNELLI, Neuri. et. al. Evaluation of occupational and patient dose in cerebral angiography procedures. **Radiologia Brasileira**. v. 46, n. 6, p. (351-357), December 2013.

[24] Reference of fluoroscopy machine manual.

LICENSE